Journal Pre-proof

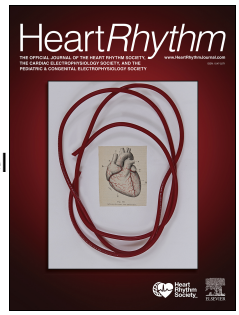

Fibroblast growth factor 21 prevents catecholaminergic arrhythmias in a mouse model of PKP2 arrhythmogenic cardiomyopathy

Xianming Lin, Noah Davidsohn, Sarah Boyce, Maritza McIntyre, Mingliang Zhang, Deborah D. Ascheim, Mario Delmar, Marina Cerrone

PII: S1547-5271(26)00153-0

DOI: https://doi.org/10.1016/j.hrthm.2026.02.030

Reference: HRTHM 11788

To appear in: *Heart Rhythm*

Received Date: 19 November 2025

Revised Date: 30 January 2026

Accepted Date: 11 February 2026

Please cite this article as: Lin X, Davidsohn N, Boyce S, McIntyre M, Zhang M, Ascheim DD, Delmar M, Cerrone M, Fibroblast growth factor 21 prevents catecholaminergic arrhythmias in a mouse model of PKP2 arrhythmogenic cardiomyopathy *Heart Rhythm* (2026), doi: https://doi.org/10.1016/j.hrthm.2026.02.030.

CENTRAL ILLUSTRATION: AAV8-FGF21 gene therapy on PKP2-cKO mice can rescue intracellular calcium imbalance, decrease the occurrence of adrenergic arrhythmias and improve the cardiac function.

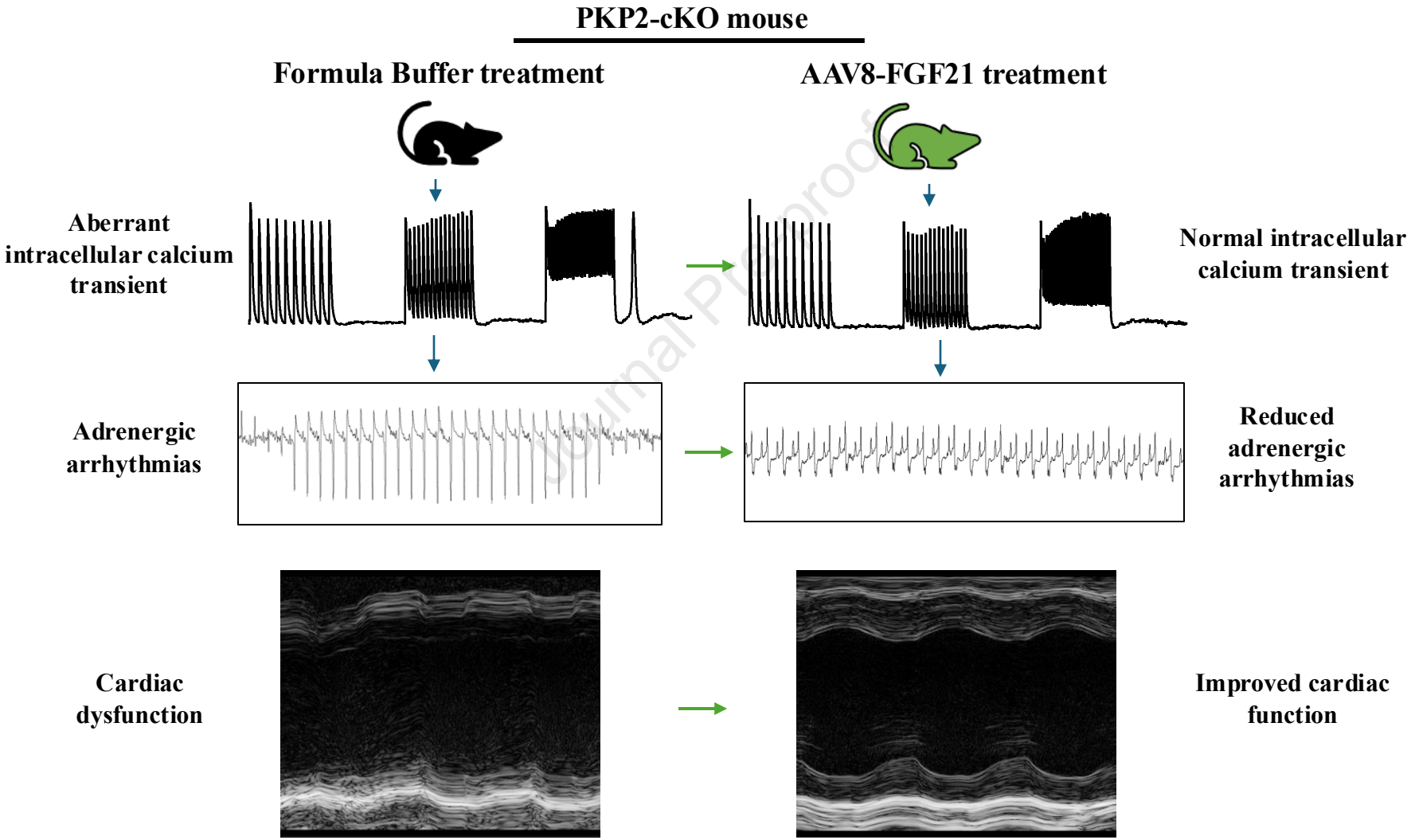

Fibroblast growth factor 21 prevents catecholaminergic arrhythmias in a mouse model of PKP2 arrhythmogenic cardiomyopathy

Xianming Lin[a], Noah Davidsohn[b], Sarah Boyce[a], Maritza McIntyre[b], Mingliang Zhang[a], Deborah D. Ascheim[b], Mario Delmar[a] and Marina Cerrone[a]

a: New York University Grossmann School of Medicine, 550 1st ave, New York, NY 10016

b: Rejuvenate Bio, 270 N El Camino Real, STE F451 Encinitas, CA 92024

Running title: FGF21 prevents catecholaminergic arrhythmias in PKP2-ACM

DISCLOSURES

There are no past, present or future royalty obligations for MD, MC, XL, MZ and SB.
ND and DDA were employees of Rejuvenate Bio at the time of study design, data collection and analysis and as such received a salary and equity. DDA and MM are consultants for Rejuvenate Bio and receive consultant fees and equity.

Correspondence to:

Marina Cerrone, MD
Research Associate Professor of Medicine
Leon H. Charney Division of Cardiology,
New York University Grossmann School of Medicine
Science Building 435 E.30th Street 712
Email: marina.cerrone@nyulangone.org

Word Count: 5513 words

Abstract

Background: Pathogenic variants in plakophilin-2 (PKP2) cause arrhythmogenic cardiomyopathy (ACM) with intracellular calcium dysregulation as a major component of its arrhythmia phenotype**.** Recent adeno‐associated viral (AAV) based *Pkp*2 (AAV-PKP2) gene therapy has shown promising results in a few different PKP2-associated ACM models. Fibroblast growth factor 21 (FGF21) has multiple cardioprotective effects and has recently emerged as a promising therapeutic agent for cardiovascular disease.

Objectives: To assess the efficacy and impact on calcium regulation of a novel AAV8-based FGF21 gene therapy on adult cardiac-specific, tamoxifen-activated PKP2 knockout (PKP2-cKO) mice.

Methods: Experiments were performed using a PKP2-cKO murine model. AAV8-FGF21 was delivered to adult mice by a single tail vein injection 7 days before tamoxifen-activated PKP2-cKO. Cardiac functions were monitored by echocardiography and electrocardiography. Intracellular calcium transients were investigated in acute isolated adult mouse cardiomyocytes and calcium fluorescent signals were acquired with the IonOptix system.

Results: Loss of PKP2 expression caused cardiac mechanical dysfunction and pro-arrhythmic phenotype in adult mouse models. AAV-mediated delivery of FGF21 mitigated the progression of biventricular structural changes, decreased the occurrence of adrenergic arrhythmias, and rescued intracellular calcium imbalance in the setting of PKP2 haploinsufficiency. In contrast, acute *in vitro* FGF21 treatment for 1 hour had no effect on intracellular calcium transients.

Conclusions: These beneficial effects of AAV8-FGF21 on the PKP2-ACM phenotype suggest a therapeutic landscape for various targeted cardiomyopathies.

Key words: arrhythmogenic right ventricular cardiomyopathy; plakophilin-2; Fibroblast growth factor 21; gene therapy; adeno-associated virus; intracellular calcium regulation.

Abbreviations

ACM, arrhythmogenic cardiomyopathy; PKP2, plakophilin-2; AAV, adeno-associated virus; FGF, Fibroblast growth factor; FB, formulation buffer; PVC, premature ventricular contraction; LVEF, left ventricular ejection fraction; FS, Fractional shortening; DCT, delayed calcium transient; dpi, days post injection.

INTRODUCTION

Arrhythmogenic cardiomyopathy (ACM) is an inherited heart disease that can result in arrhythmias, sudden cardiac death, progressive fibrofatty replacement of the myocardium and heart failure. Pathogenic variants of genes encoding desmosome proteins account for more than 50% of familial cases, with the majority being plakophilin-2 (*Pkp2*) gene variants. [1] Currently, there is no available targeted treatment, and antiarrhythmic medications do not offer protection to all patients. Recently cardiac targeted adeno-associated viral (AAV) based *Pkp2* (AAV-PKP2) gene replacement therapy has shown promising results in three different PKP2-associated ACM mouse models and in human-induced pluripotent stem cell-derived cardiomyocytes (*h*iPSC-CMs).[2-5] Specifically, data show that AAV-PKP2 therapy can prevent the development of ACM when administered prior to the onset of overt cardiomyopathy or delay disease progression when given after the emergence of symptoms. [2-5] However, this specific gene therapy is so far limited to PKP2-associated cardiomyopathy, and its efficacy may not extend to other forms of cardiomyopathies caused by different genetic drivers.

Fibroblast growth factors (FGFs) are well characterized and have a broad range of regulatory functions in embryonic development, tissue repair, regeneration, and metabolism. [6] There are at least 22 different FGFs, categorized amongst 7 subfamilies; among them, FGF21 is a stress inducible hormone member of the FGF19 subfamily, and it is produced in multiple organs, including the liver, adipose tissue, skeletal muscle, pancreas, and heart. [7] FGF21 serum levels can increase in response to cardiac stress, indicating that it could be a potential biomarker for cardiovascular disease. [8-11] This elevation is often associated with an FGF21 resistive state, where the expression of FGF receptors (FGFR) or its co-receptor β-Klotho is reduced, leading to a compensatory cascade. [11,12]

Studies show that FGF21 can prevent cardiac oxidative stress, hypertrophy, metabolic disorder and inflammation. These cardioprotective effects have been demonstrated in multiple animal models and *in vitro* studies. [8,13] However, the native FGF21 protein has a short half-life (0.5~2 hours) and is unsuitable for clinical use. To address this pharmacokinetic limitation, long-acting FGF21 analogues which can increase stability and applicability have been developed and several FGF21 analogues and mimetics have been tested in different phases of clinical trials. [14-16] Recently, an AAV based gene therapy of FGF21 (AAV-FGF21) which can mediate long-term transgene production of FGF21 has been developed to treat obesity, insulin resistance, type 2 diabetes, and associated cognitive decline. [17,18]

Given the cardioprotective effect of FGF21 and the effectiveness of AAV-FGF21, in the present study we test the effects of a novel AAV8-FGF21 vector on adult cardiac-specific, tamoxifen-activated PKP2 knockout (PKP2-cKO) mice in which the loss of PKP2 expression leads to ACM with aberrant intracellular calcium transient, contractile dysfunction, cardiac fibrosis and progression to end-stage heart failure and death.[19] Our experiments show that AAV8 mediated delivery of FGF21 can mitigate arrhythmias and decline in ventricular function in a mouse model with PKP2 haploinsufficiency.

METHODS

Animals

Animal experiments were performed in 3–4-month-old cardiac-specific, tamoxifen-activated PKP2 knockout (PKP2-cKO) mice. [19] Experiments were conducted at 21- or 28-days post injection (dpi) of tamoxifen (TAM). Procedures conformed with the Guide for Care and Use of Laboratory Animals of the National Institutes of Health and were approved by the New York University Institutional Animal Care and Use Committee (160 726-03).

Administration of AAV vector

Administration of an intended volume of 100 µL of AAV8-murine FGF21 ($1.5x10^{13}$ vg/kg), or formulation buffer (FB), was performed by a single tail vein injection at 7 days before TAM injection in the PKP2-cKO mice. Before treatment, fresh samples of AAV8-FGF21 and FB were prepared to generate the appropriate concentration and maintained on wet ice. A group of 9 PKP2-cKO mice received AAV8-murine FGF21 by a single tail injection 7 days after TAM injection. The operators (administration and in vivo/in vitro characterization) were blinded to the content of each specific vector and respective group treatments were only revealed at the end of data analysis.

Serum FGF21 concentration measurements

Serum FGF21 concentrations were determined using the Mouse FGF-21 SimpleStep ELISA kit (Abcam, ab212160) following the manufacturer's instructions with minor modification. Blood was collected into serum separator tubes, allowed to clot at room temperature, and centrifuged at 2,000 × g for 10 min to isolate serum. Samples were stored at −80 °C and thawed immediately prior to analysis. On the day of assay, serum was diluted 1:250 in the provided assay diluent. An eight-point standard curve (9.375–600 pg ml^{-1}) was prepared in parallel, and 100 µl of diluted samples, standards, and blanks were added to wells pre-coated with capture

antibody in the SimpleStep format. After incubation with the antibody cocktail, wells were washed once, developed with tetramethylbenzidine substrate, and stopped with the supplied solution. Absorbance was measured at 450 nm on a microplate reader, and concentrations were interpolated from a four-parameter logistic fit of the standard curve, with final values adjusted for the dilution factor. All samples and standards were run in duplicate.

Electrocardiogram recordings

Electrocardiogram (ECG) recordings were performed on PKP2-cKO mice injected with either AAV8-FGF21 or FB as well as FB-injected Cre-negative mice 21 days post-tamoxifen injection as previously described [19] Mice were anesthetized with 1.5% isoflurane in 700 ml O_2 per minute via a nose cone (following induction in a chamber containing 3-4% isoflurane in O_2) for the duration of the procedure. Rectal temperature was maintained at 37-38 °C. ECG (leads I, II, III) was recorded via subcutaneous needle electrodes inserted in each limb. The first 1-3 minutes of the recording were used for stabilization. Mice were then injected with 3 mg/kg isoproterenol (ISO) intraperitoneally as a single bolus and ECG was recorded for another 30 min following ISO injection. The analysis was performed on LabChart 7.0-Pro software. To calculate ISO challenge arrhythmic burden, the number of premature ventricular contractions (PVCs) was quantified manually and confirmed by a second operator.

Echocardiography

Echocardiography was performed on AAV-FGF21-injected, FB-injected PKP2-cKO mice, and on FB injected flox/flox Cre-negative mice at 28 dpi using a Vevo 2100 machine (Visualsonics Inc) as described in Cerrone et al. [19] Body temperature was maintained at 36.5-37ºC, Quantitative measurements were analyzed using the Vevo2100 analytical software. The left ventricular ejection fraction (LVEF, %) was calculated using B-mode parasternal long axis view and volume measures using the proprietary Visualsonics Inc. software (vsi_cardiac

package.sxml). Fractional shortening (FS) was measured from the M-mode short axis view. The right ventricular (RV) area was calculated using the B-Mode modified parasternal long axis view of the RV to visualize the chamber and determine the RV diameter measured halfway between the pulmonary and tricuspid valves from the interventricular septum to the free wall during diastole.

Masson's Trichrome staining

Following extraction, hearts were fixed in 4% paraformaldehyde in PBS overnight, embedded in paraffin, and cut into sections 5μm thick. Sections were stained using Masson's Trichrome staining kit, according to the manufacturer's instructions (Plysciences 25088). The sections were heated at 60 °C for 30 min and rehydrated. Slides were then incubated in Bouin's solution, 60 °C for 1 h followed by wash steps and immersed in Weigert's working hematoxylin solution for 10 min. After washes, slides were immersed in Biebrich Scarlet–Acid Fuchsin solution for 5 min and phosphomolybdic acid solution for 10 min prior to Aniline blue incubation for 5 min. Slides were then incubated in 1% acetic acid for 1 min, rinsed, dehydrated and mounted with Permount Mounting Medium. Stained sections were scanned at a 10x magnification using a Keyence All-in-One Fluorescence Microscope (BZ-X800E, Keyence, NJ, USA). The ImageJ (NIH) software was used for analysis of tissue sections, as previously described. [19] Six to seven regions of interest (ROIs) for each ventricle were identified and the interventricular septum was excluded. Percentage Fibrosis was measured as the area of collagen (blue staining) normalized to the area of tissue in the ROI.

***In vitro* experiments with FGF21**

To minimize the lack of FGF21 exposure between *in-vivo* and *in-vitro* transfer of the myocardium and prevent the washout of FGF21 that was in the circulation of the mouse, 50 ng/ml recombinant mouse FGF21 (rmFGF21) protein (Catalog #: 8409-FG; RD systems;

Minneapolis, MN, USA) or formulation buffer (FB) were added to all the solutions utilized for cardiomyocyte dissociation and calcium transient experiments. 50 ng/ml rmFGF21 were also used for 1 hour incubation with the isolated cardiomyocytes to test the acute effect of FGF21 on intracellular calcium transients.

Cardiomyocyte dissociation

Adult female mouse ventricular myocytes were obtained by enzymatic dissociation. Briefly, mice were injected with 0.1 ml heparin (500 IU/ml intraperitoneally) 10 min before heart excision and anaesthetized by inhalation of 100% CO_2. When deep anesthesia was confirmed, mice were killed by cervical dislocation and the heart was surgically removed from the chest and placed in a Langendorff column. For cell dissociation, the isolated hearts were perfused sequentially with low calcium, and an enzyme (collagenase, Worthington) solution maintained at 37°C. After digestion, ventricles were cut into small pieces and gently minced with a Pasteur pipette. Calcium concentration increased gradually to 1.0 mM. Cardiomyocytes were kept in Tyrode's solution containing (in mM): 148 NaCl, 5.4 KCl, 1.0 $MgCl_2$, 1.0 $CaCl_2$, 0.4 NaH_2PO_4, 15 HEPES and 5.5 glucose, pH 7.40. Cells were used within 3h after isolation.

Calcium imaging

Isolated mouse ventricular myocytes were loaded for 12 min with Fluo-8/AM (Invitrogen Inc., Eugene, OR, USA) in Tyrode's solution containing (in mM): 140 NaCl, 4 KCl, 2.0 $CaCl_2$, 1 $MgCl_2$, 10 Hepes and 5.6 glucose followed by a 30 min wash in Tyrode's solution. Fluorescent signals were acquired with the IonOptix system (IonOptix Corp., Milton, MA, USA). Cells were paced at 1 Hz to achieve steady state, then paced for 15 seconds at different rates (0.5-1-3 Hz) with 15 seconds resting interval between different rates. Following background subtractions, data were calculated as the ratio of Fluo-8 fluorescence intensity over baseline (F/F0). The calcium transient traces at 1 Hz were analyzed using IonWizard (IonOptix) to

determine the time to peak, decay time constants and calcium transient peak amplitude. Intracellular calcium transients were recorded from 18-25 cardiomyocytes per heart. An unprovoked calcium transient recorded during the first 15 seconds after a pacing train of 15 seconds at 3 Hz was classified as a delayed calcium transient (DCT). The DCT ratio refers to the number of cells that manifest DCTs divided by the total number of cells recorded for each individual heart.

Statistical analysis

Numerical results are given as mean and standard deviation (mean ± SD). For cardiomyocyte calcium transient data obtained from more than one mouse within a group, the SPSS mixed model analysis was used, as specified in the figure legends. All other data sets were tested for normal distribution by the Shapiro–Wilk and Kolmogorov–Smirnov tests. Significance was determined by parametric or non-parametric methods (GraphPad Prism v.9.4.1), as appropriate. Statistical significance was set for p values < 0.05.

RESULTS

The AAV8-FGF21 vector was administered 7 days before TAM injection in the PKP2-cKO mice to allow sufficient transgene expression before assessing its effects on the ACM phenotype at 21 and 28 dpi respectively (Figure 1). Serum FGF21 levels in vector-injected mice were measured every two weeks, starting 14 days after injection (T0). As shown in Figure 1, FGF21 levels could be detected 14 days post injection (dpi) and continued to increase up to the last test time point at 42 dpi.

An ISO challenge (3 mg/kg ip, single bolus) can elicit premature ventricular contractions (PVC) and ventricular arrhythmias in anesthetized PKP2-cKO mice 21 days after tamoxifen injection. [19] Here, we sought to determine if AAV8-FGF21 could prevent the occurrence of ISO-induced arrhythmias. As shown in Figure 2A-B, FB-treated PKP2-cKO (labelled "KO FB" in Figure 2) had a high PVC burden, while mice pre-treated with AAV8-FGF21 (KO AAV in Figure 2) showed a significant reduction in the incidence of ectopic beats (Figure 2A). Importantly, none of the treated animals showed a high arrhythmia burden, defined as PVC count >100, in contrast with what is seen in the majority of untreated PKP2cKO animals (Figure 2B; 6 of 8 and 0 of 8 for KO FB and KO AAV, respectively). Exemplary ECG traces are shown in Figure 2C.

Echocardiography was performed in FB- or AAV8-FGF21- injected PKP2-cKO mice 28 days after tamoxifen injection. As shown by the examples presented in Figure 3A, and the summary data in Figures 3B-D, FB-treated animals (n=8) showed the expected reduced left ventricular ejection fraction (LVEF; 3B), fractional shortening (FS; 3C) and increased right ventricular dimensions (RV area; 3D) at 28 dpi (data in red columns, labelled "KO FB"). [19] In contrast, LVEF and FS values in PKP2-cKO mice treated with AAV8-FGF21 were significantly higher and close to normal values (data in blue columns, labelled "KO AAV." Data from a control,

FB-injected group in grey bars, labelled “CTRL FB”). RV dimensions in the AAV8-FGF21 group were also smaller than those in PKP2-cKO mice injected with FB, and not different from Cre-controls (CTRL FB) ($p = 0.259$). Gene therapy with FGF21 also tended to mitigate the extent of fibrosis measured by Trichrome staining in both the right and the left ventricle of most mice, yet given data variability, the results collected from treated PKP2-cKO animals were not statistically different from those collected from FB-treated animals (Fig 3E-G).

We also tested the effect of AAV8-FGF21 administered 7 days after TAM injection (i.e. after PKP2 loss but before the onset of overt cardiomyopathy) on arrhythmias and cardiac function in a group of PKP2-cKO mice. Gene therapy with FGF21 significantly maintained LVEF and FS values (Fig.4A and 4B), RV area dimensions (4C) and prevented the occurrence of ISO-mediated arrhythmias (4D-E) when compared with FB-treated PKP2-cKO animals.

We previously showed that intracellular calcium dysregulation is a feature of PKP2-cKO cardiomyocytes [19] and likely a major component of their arrhythmia phenotype. We therefore investigated the effect of AAV8-FGF21 treatment on calcium dysregulation in PKP2-cKO mice. For these experiments, cardiomyocytes were derived by female hearts only, based on previous observations that the PKP2-cKO model does not show sex differences in disease features and progression.[20]

Calcium transients recorded from 4 separate cardiomyocytes, each paced at 1 Hz, are shown in Figure 5A. As expected, calcium transients in PKP2-cKO cardiomyocytes (in this case, from mice injected with FB; labelled KO FB; red trace in 5A-left) showed a larger amplitude and prolonged decay time constant when compared to a control (5A, left panel; black trace; labelled Ctrl FB). The data on decay time constant and amplitude are summarized in Figures 5B-C, respectively. The values of calcium transient amplitude, decay time constant and time to peak from individual cell are presented in Supplemental Figure 1. In agreement with our previous

studies, [19] there was also increased occurrence of delayed calcium transients (DCTs) in FB injected PKP2-cKO cardiomyocytes (exemplary traces in Figure 5D; data summarized in 5E). AAV8-FGF21 counteracted the effect of PKP2 deficiency on the cardiomyocyte intracellular calcium transient decay time constant and peak amplitude (exemplary traces in Figure 5A, right; data in 5B-C; compare "KO FB" in red bar to "KO AAV" in blue bar). As shown in Fig.5E, AAV8-FGF21 injection also reduced the average DCTs ratio from 50.6 ± 8.8% (red bar; n=6 hearts) to 37.0 ± 10.9% (blue bar; n=6 hearts). These results suggest that the antiarrhythmic effect of FGF21 shown in Figure 2 may result, at least in part, from its effects on mitigating intracellular calcium dysregulation.

The intracellular calcium imaging experiments described above were obtained from myocytes isolated from PKP2-cKO hearts. In the case of AAV8-FGF21-injected animals, cardiac exposure to FGF21 occurred via the circulating FGF21 in the blood, but a time gap of no-FGF21-exposure existed between the extraction of the heart from the chest of the animal, and the time of recording (approximately 2 hours; data from this group is shown as "KO AAV" in the blue bars of Figure 5). To minimize this no-exposure gap, separate experiments were conducted where 50 ng/ml FGF21 were added to all solutions utilized through the dissociation steps, incubation, and recording (data KO AAV+FGF; gray trace in Figure 5A-right and gray bars in Figure 5B-C and 5E). As shown in Figure 5 the effect of FGF21 was further enhanced by this supplementation, although there was no change in the DCTs occurrence ratio (Figure 5E). Yet, it is important to note that acutely exposing cardiomyocytes to FGF21 did not have an effect on calcium transient parameters, regardless of whether the cells were dissociated from a control (Figure 6A-D) or a PKP2cKO heart (Figure 6E-H). Taken together, these results suggest that the beneficial effect of AAV8-FGF21 injection on arrhythmogenesis are not consequent to a direct and acute regulation of intracellular calcium homeostasis in cardiomyocytes.

DISCUSSION

The present study provides pharmacological evidence that adenovirus-mediated FGF21 gene delivery by a single tail vein injection can decrease the occurrence of adrenergic arrhythmias, mitigate the progression of structural changes in both ventricles, and rescue intracellular calcium imbalance in the setting of PKP2 haploinsufficiency. These beneficial effects on the PKP2-ACM phenotype occur in the absence of direct gene replacement therapy, opening the possibility that other genetic forms of ACM could benefit from this treatment.

AAV serotypes have been used for gene delivery due to their non-pathogenicity in humans and long-lasting expression. Previous studies have shown that after a single tail vein injection in mice, AAV8 mediated expression can be localized to various target organs, such as liver, skeletal muscle and heart in less than 7 days after delivery and peaked at 56 dpi. [21] The expression cassette delivered by AAV8 in this study restricted FGF21 expression to the liver. Therefore, the cardiac benefits of AAV8 mediated gene therapy observed in this study most likely result from circulating exogenous FGF21 secreted from the liver. [22,23]

In the present study, we have demonstrated that the PKP2cKO hearts benefit from systemic (and prolonged) administration of FGF21. Yet, the primary cell target remains to be defined. There are multiple cell populations forming cardiac parenchyma, and substantial intercellular crosstalk is likely to occur. Our observation that adding 50 ng/ml FGF21 during the cell dissociation step can further help normalize intracellular calcium homeostasis, while acute FGF21 exposure on isolated cardiomyocyte has no effect, suggest that cardiac cells, but not necessarily (or not only) myocytes, are key mediators of the FGF21 beneficial effect. In that context, it is important to note that FGF21 can inhibit fibroblast proliferation and differentiation and ameliorate cardiac fibrosis. FGF21 can also target macrophages in the heart where β-Klotho is expressed and exert an anti-inflammatory effect. [24] Finally, through specific

intracellular signaling cascades, [25,26] FGF21 may stabilize mitochondrial homeostasis under oxidative stress, hence limiting ROS production. [26] Mitochondrial dysfunction and a pro-fibrotic, pro-inflammatory molecular phenotype can contribute to mechanical dysfunction and intracellular calcium dysregulation and are reported to occur in patients with ACM and in animal models of disease. [27] The intimate mechanisms by which FGF21 bring about the improvements on the PKP2-ACM phenotype described here remain an important area of future investigation.

Four different groups have demonstrated efficacy with AAV9-based PKP2 gene therapy. [2-5] These studies, however, focused on introducing a "healthy" PKP2 gene to compensate for the loss of function of a missing or mutated allele. As such, PKP2 gene replacement therapy is restricted to PKP2-associated ARVC cases. Our results lead us to speculate that FGF21 gene therapy can be a genotype independent approach for treating ACM, including those that are found to be gene-negative.[1] Indeed, basic science studies on models of different forms of desmosomal ARVC, including *PKP2* , *DSG2* and *DSP* deficiency converge on similar mechanisms involving mitochondrial dysfunction, a pro-inflammatory, auto-immune response and in those studied, calcium dysregulation.[20, 28-33] We surmise that treatments that impact these or other common factors would have a benefit in a relatively gene-agnostic manner.

It is also unclear whether AAV-FGF21 therapy can reverse symptoms and halt the disease progression for ARVC with late-stage administration. The present results provide pre-clinical evidence to support further experimentation that can lead, if successful, to clinical trials to evaluate its safety and effectiveness in patients with ACM.

In conclusion, our study demonstrates that AAV8-FGF21 gene therapy mitigates the structural and mechanical dysfunction, as well as the pro-arrhythmic phenotype observed in PKP2-deficient mice. We further show that the reduction in arrhythmia burden associates with

improved intracellular calcium homeostasis, a main mechanism of arrhythmogenesis in PKP2-deficient hearts. By targeting a gene with broad regulatory functions rather than replacing a direct disease-causing gene, our findings pave the way for novel gene therapy strategies that may encompass arrhythmogenic cardiomyopathies beyond the narrow field of PKP2-ACM. These approaches may be particularly valuable for inherited cardiomyopathies with unknown genetic causes or limited treatment options, offering a promising direction for future therapeutic development.

SOURCES OF FUNDING
Supported through a sponsored research agreement between Rejuvenate Bio and NYU Grossman School of Medicine.

DISCLOSURES
There are no past, present or future royalty obligations for MD, MC, XL, MZ and SB. ND and DDA were employees of Rejuvenate Bio at the time of study design, data collection and analysis and as such received a salary and equity. DDA and MM are consultants for Rejuvenate Bio and receive consultant fees and equity.

REFERENCES

1. Gandjbakhch E, Redheuil A, Pousset F, Charron P, Frank R. Clinical Diagnosis, Imaging, and Genetics of Arrhythmogenic Right Ventricular Cardiomyopathy/Dysplasia: JACC State-of-the-Art Review. *J Am Coll Cardiol*. 2018;72:784-804.

2. Kyriakopoulou E, Versteeg D, de Ruiter H, et al. Therapeutic efficacy of AAV-mediated restoration of PKP2 in arrhythmogenic cardiomyopathy. *Nat Cardiovasc Res*. 2023;2:1262-1276.

3. Wu I, Zeng A, Greer-Short A, et al. AAV9:PKP2 improves heart function and survival in a Pkp2-deficient mouse model of arrhythmogenic right ventricular cardiomyopathy. *Commun Med (Lond)*. 2024;4:38. doi: 10.1038/s43856-024-00450-w.

4. van Opbergen CJM, Narayanan B, Sacramento CB, et al. AAV-Mediated Delivery of Plakophilin-2a Arrests Progression of Arrhythmogenic Right Ventricular Cardiomyopathy in Murine Hearts: Preclinical Evidence Supporting Gene Therapy in Humans. *Circ Genom Precis Med*. 2024;17:e004305. doi: 10.1161/CIRCGEN.123.004305.

5. Bradford WH, Zhang J, Gutierrez-Lara EJ, et al. Plakophilin 2 gene therapy prevents and rescues arrhythmogenic right ventricular cardiomyopathy in a mouse model harboring patient genetics. *Nat Cardiovasc Res*. 2023;2:1246-1261.

6. Ornitz DM, Itoh N. The Fibroblast Growth Factor signaling pathway. *Wiley Interdiscip Rev Dev Biol*. 2015;4:215-266.

7. Wang XP, Xing CY, Zhang JX, et al. Time-restricted feeding alleviates cardiac dysfunction induced by simulated microgravity via restoring cardiac FGF21 signaling. *FASEB J*. 2020;34:15180-15196.

8. Planavila A, Redondo-Angulo I, Villarroya F. FGF21 and Cardiac Physiopathology. *Front Endocrinol (Lausanne)*. 2015;6:133. doi: 10.3389/fendo.2015.00133.

9. Zhang Y, Yan J, Yang N, et al. High-Level serum Fibroblast Growth Factor 21 concentration is closely associated with an increased risk of cardiovascular diseases: A systematic review and Meta-Analysis. *Front Cardiovasc Med*. 2021;8:705273. doi: 10.3389/fcvm.2021.705273.

10. Chou RH, Huang PH, Hsu CY, et al. Circulating Fibroblast Growth Factor 21 is Associated with Diastolic Dysfunction in Heart Failure Patients with Preserved Ejection Fraction. Sci Rep. 2016;6:33953. doi: 10.1038/srep33953.

11. Tucker W, Tucker B, Rye KA, Ong KL. Fibroblast growth factor 21 in heart failure. *Heart Fail Rev*. 2023;28:261-272.

12. Patel V, Adya R, Chen J, et al. Novel insights into the cardio-protective effects of FGF21 in lean and obese rat hearts. *PLoS One*. 2014;9:e87102. doi: 10.1371/journal.pone.0087102.

13. Planavila A, Redondo I, Hondares E, et al. Fibroblast growth factor 21 protects against cardiac hypertrophy in mice. *Nat Commun*. 2013;4:2019. doi: 10.1038/ncomms3019.

14. Shao W, Jin T. Hepatic hormone FGF21 and its analogues in clinical trials. *Chronic Dis Transl Med*. 2022;8:19-25.

15. Gaich G, Chien JY, Fu H, et al. The effects of LY2405319, an FGF21 analog, in obese human subjects with type 2 diabetes. *Cell Metab*. 2013;18:333-340.

16. Talukdar S, Zhou Y, Li D, et al. A Long-Acting FGF21 molecule, PF-05231023, decreases body weight and improves lipid profile in non-human primates and type 2 diabetic subjects. *Cell Metab*. 2016;23:427-440.

17. Jimenez V, Jambrina C, Casana E, et al. FGF21 gene therapy as treatment for obesity and insulin resistance. *EMBO Mol Med*. 2018;10:e8791. doi: 10.15252/emmm.201708791.

18. Kakoty V, C SK, Yang CH, et al. Neuroprotective effect of lentivirus-mediated FGF21 gene delivery in experimental Alzheimer's disease is augmented when concerted with rapamycin. *Mol Neurobiol*. 2022;59:2659-2677.

19. Cerrone M, Montnach J, Lin X, et al. Plakophilin-2 is required for transcription of genes that control calcium cycling and cardiac rhythm. *Nat Commun.* 2017;8(1):106. doi: 10.1038/s41467-017-00127-0.

20. Pérez-Hernández M, van Opbergen CJM, Bagwan N, et al. Loss of Nuclear Envelope Integrity and Increased Oxidant Production Cause DNA Damage in Adult Hearts Deficient in PKP2: A Molecular Substrate of ARVC. *Circulation*. 2022;146(11):851-867. doi: 10.1161/CIRCULATIONAHA.122.060454.

21. Zincarelli C, Soltys S, Rengo G, Rabinowitz JE. Analysis of AAV serotypes 1-9 mediated gene expression and tropism in mice after systemic injection. *Mol Ther*. 2008;16:1073-1080.

22. Sommakia S, Almaw NH, Lee SH, et al. FGF21 (Fibroblast Growth Factor 21) defines a potential cardiohepatic signaling circuit in end-stage heart failure. *Circ Heart Fail*. 2022;15:e008910. doi: 10.1161/CIRCHEARTFAILURE.121.008910.

23. Markan KR, Naber MC, Ameka MK, et al. Circulating FGF21 is liver derived and enhances glucose uptake during refeeding and overfeeding. *Diabetes*. 2014;63:4057-4063.

24. Yu Y, He J, Li S, et al. Fibroblast growth factor 21 (FGF21) inhibits macrophage-mediated inflammation by activating Nrf2 and suppressing the NF-κB signaling pathway. *Int Immunopharmacol*. 2016;38:144-152.

25. Zhang C, Huang Z, Gu J, et al. Fibroblast growth factor 21 protects the heart from apoptosis in a diabetic mouse model via extracellular signal-regulated kinase 1/2-dependent signalling pathway. *Diabetologia*. 2015;58:1937-1948.

26. Yan B, Mei Z, Tang Y, et al. FGF21-FGFR1 controls mitochondrial homeostasis in cardiomyocytes by modulating the degradation of OPA1. *Cell Death Dis*. 2023;14:311. doi: 10.1038/s41419-023-05842-9.

27. van Opbergen CJM, den Braven L, Delmar M, van Veen TAB. Mitochondrial dysfunction as substrate for arrhythmogenic cardiomyopathy: A search for new disease mechanisms. *Front Physiol*. 2019;10:1496. doi: 10.3389/fphys.2019.01496.

28. Martini M, Parodi A, Marinas MB, et al. Hot phase episodes in Arrhythmogenic cardiomyopathy: More than just a Desmoplakin issue? *Trends Cardiovasc Med*. 2025:S1050-1738(25)00163-X. doi: 10.1016/j.tcm.2025.12.005.

29. Penna VR, Amrute JM, Engel M, et al. Interleukin-1β Drives Disease Progression in Arrhythmogenic Cardiomyopathy. *bioRxiv [Preprint]*. 2024:2024.12.11.628020. doi: 10.1101/2024.12.11.628020.

30. Olcum M, Rouhi L, Fan S, et al. PANoptosis is a prominent feature of desmoplakin cardiomyopathy. *J Cardiovasc Aging*. 2023;3(1):3. doi: 10.20517/jca.2022.34.

31. Pérez-Hernández M, Marrón-Liñares GM, Schlamp F, et al. Transcriptomic Coupling of PKP2 With Inflammatory and Immune Pathways Endogenous to Adult Cardiac Myocytes. *Front Physiol*. 2021;11:623190. doi: 10.3389/fphys.2020.623190.

32. Kim JC, Pérez-Hernández M, Alvarado FJ, et al. Disruption of Ca2+i Homeostasis and Connexin 43 Hemichannel Function in the Right Ventricle Precedes Overt Arrhythmogenic

Cardiomyopathy in Plakophilin-2-Deficient Mice. *Circulation*. 2019;140(12):1015-1030. doi: 10.1161/CIRCULATIONAHA.119.039710.

33. van Opbergen CJM, Bagwan N, Maurya SR, et al. Exercise Causes Arrhythmogenic Remodeling of Intracellular Calcium Dynamics in Plakophilin-2-Deficient Hearts. *Circulation*. 2022;145(19):1480-1496. doi: 10.1161/CIRCULATIONAHA.121.057757.

Figure legends

Figure 1. Study design and the AAV-mediated FGF21 expression over time. Visual representation of the study design alongside FGF21 expression overtime. Mice were injected with AAV8-FGF21 7 days before tamoxifen injection, with day 0 being knockout induction by tamoxifen injection. 21 days post-TAM, mice underwent an isoproterenol challenge with ECG recording. On day 28-post TAM, an echocardiography was performed, followed by euthanasia and heart collection. FGF21 levels achieved the maximum expression at 42 dpi and the serum FGF21 protein concentration is 27.4±10.9 ng/ml (n=9).

Figure 2. Quantitative analysis of electrocardiogram (ECG). **A**, AAV8-FGF21 injection significantly reduced PKP2-deficiency induced arrhythmias following isoproterenol challenge (3 mg/kg intraperitoneally), as evidenced by decreased incidence and severity of ventricular arrhythmias manifest by premature ventricular contractions (PVC) burden in AAV8-FGF21 treated PKP2-cKO mice relative to PKP2-cKO controls. n=8 (4 male and 4 female) mice for each group. **B**, AAV8-FGF21 injection reduced the ratio of PKP2-cKO mice with >100 PVC induced by isoproterenol challenge. **C**, Representative ECG traces from PKP2-cKO mice treated with formulation buffer (KO FB) and AAV-FGF21 (KO AAV) 21 days after tamoxifen injection. Mann-Whitney unpaired t-test.

Figure 3. Echocardiography assessment of cardiac function and histological analysis of cardiac fibrosis. **A**, Representative images of left ventricular (LV) echocardiography to assess contractility in Cre-negative control mice injected with FB (Ctrl FB) and PKP2-cKO mice treated with AAV-FGF21 (KO AAV), or FB (KO FB) 28 days after tamoxifen injection. AAV-FGF21 injection enhances preservation of left ventricle ejection fraction (LVEF) (**B**) and fractional shortening (FS) (**C**) while also significantly minimizing RV dilation (**D**). **E**, Representative images of Masson trichrome staining of longitudinal heart sections of Cre-

negative control mice treated with FB (Ctrl FB) and PKP2-cKO mice treated with FB (KO FB) or AAV-FGF21 (KO AAV) 28 days after tamoxifen injection. Collagen deposition in blue. **F and G**, Quantification of the percentage of left ventricular fibrosis (B) and right ventricle fibrosis (C). N=8 (4 male and 4 female) mice for each group. Mann-Whitney unpaired t-test.

Figure 4. Echocardiographic assessment and ECG analysis of the effect of AAV8-FGF21 administered 7 days after tamoxifen injection. AAV-FGF21 injection preserves left ventricle ejection fraction (LVEF) (**A**) and fractional shortening (FS) (**B**) while also significantly minimizing RV dilation (**C)** at 28 days post tamoxifen injection (n=10 PKP2cKO-FB and n=9 PKP2cKO-AAV animals). AAV-FGF21 injection mitigated the burden of premature ventricular contractions (PVCs) after 3mg/Kg isoproterenol (ISO) injection (**D)** and reduced the ratio of PKP2-cKO mice with >100 PVC induced by ISO challenge **(E,** n=9 PKP2cKO-FB and n=8 PKP2cKO-AAV, to exclude outliers). Mann-Whitney unpaired t-test.

Figure 5. Characteristics of calcium transients recorded from cells dissociated from the hearts of adult female Cre-negative control mice injected with FB (Ctrl FB), PKP2cKO mice injected with AAV8-FGF21(KO AAV) or its formulation buffer (KO FB), and cells dissociated from female AAV8-FGF21-injected PKP2-cKO mice with 50 ng/ml FGF21 kept in all the solutions utilized through cardiomyocytes dissociation and calcium transient recording (KOAAV+FGF). **A**, example of intracellular Ca^{2+} transients recorded under the four different groups with 1 Hz Pacing rate. **B–C**, quantification of decay time constant (B) and peak amplitude (C) of calcium transients from ventricular myocytes paced at 1 Hz rate. Each dot presents the averaged value of a total of 18-25 cells studied in one animal. **D,** examples of calcium transients in three different groups with different pacing rates (0.5–1–3 Hz). Delayed calcium transients (DCTs) were recorded after 3Hz pacing. **E**, ratio of the cells with DCTs. Each dot presents the ratio of DCTs in one animal. N=5, 6, 6, and 4 mice for Ctrl FB, KO FB, KO AAV and KO AAV+FGF. Ordinary one-way ANOVA analysis.

Figure 6. Quantification of time to peak **(A and E),** decay time constant **(B and F),** and peak amplitude **(C and G)** of cardiomyocyte calcium transients at 1 Hz pacing rate. The cardiomyocyte from Cre-negative control **(A-C)** or PKP2cKO **(E-G)** female mice were incubated with FB or 50 ng/ml FGF21 for 1 hour. Each dot represents the value of one cardiomyocyte and each bar represents the data from one animal. n=18-25 cardiomyocytes for each animal and N= 3 or 4 mice for each group. SPSS Mixed model analysis. **D and H**, ratio of the cells with DCTs. Mann-Whitney unpaired t-test.

Figure 1

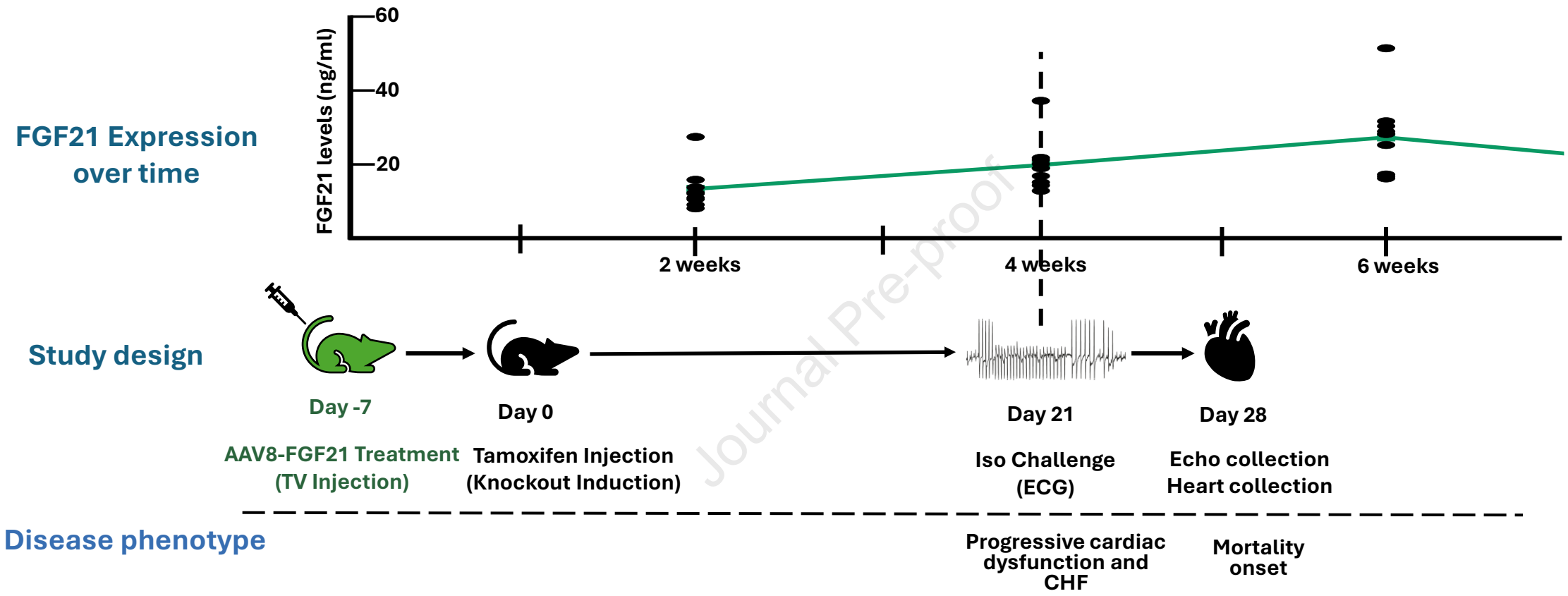

Figure 2

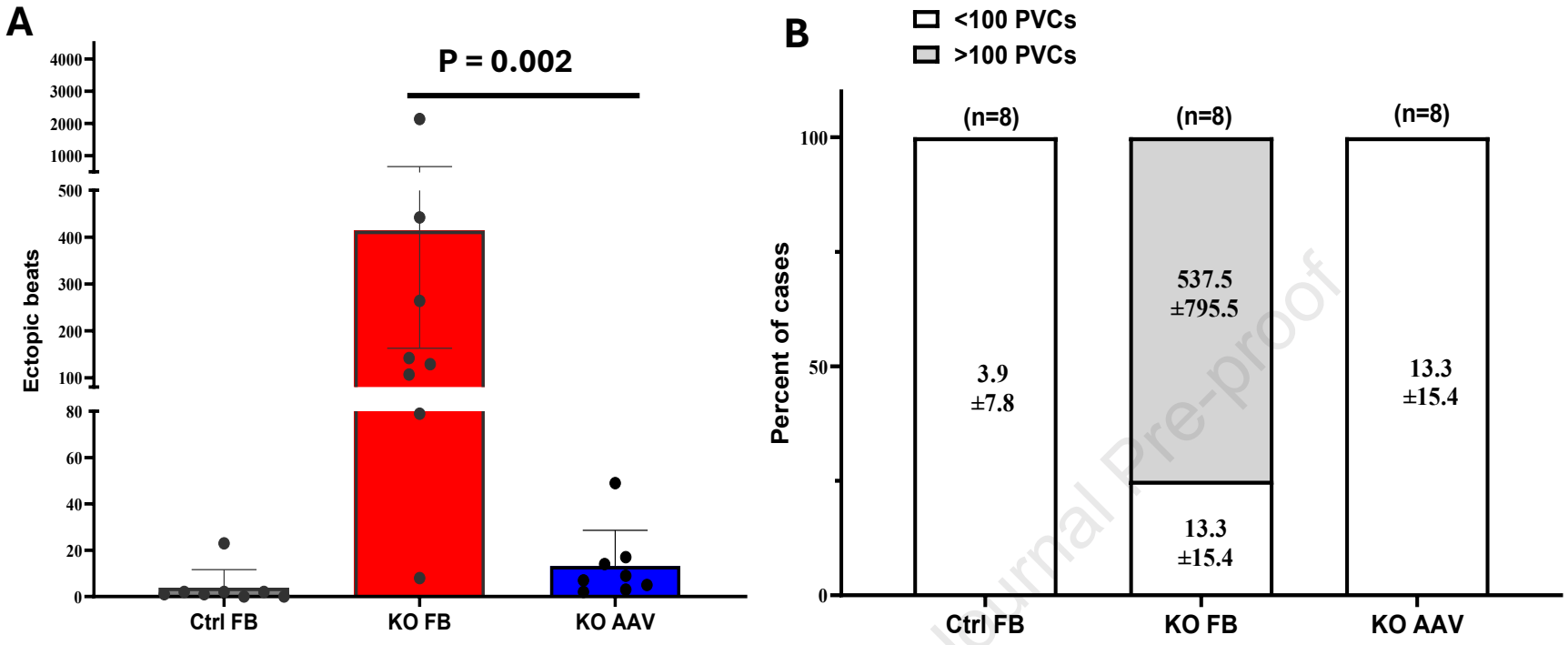

Figure 3

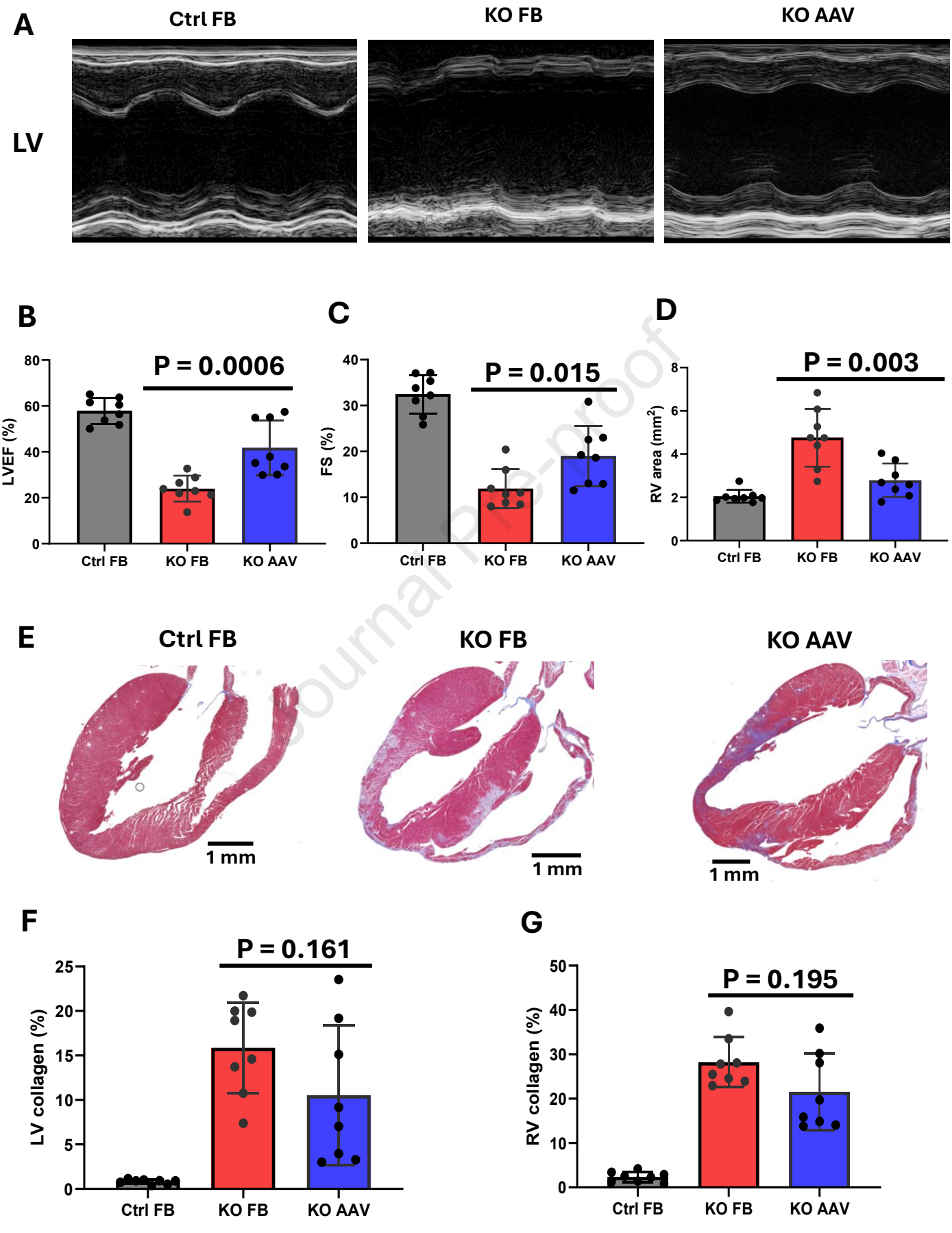

Figure 4

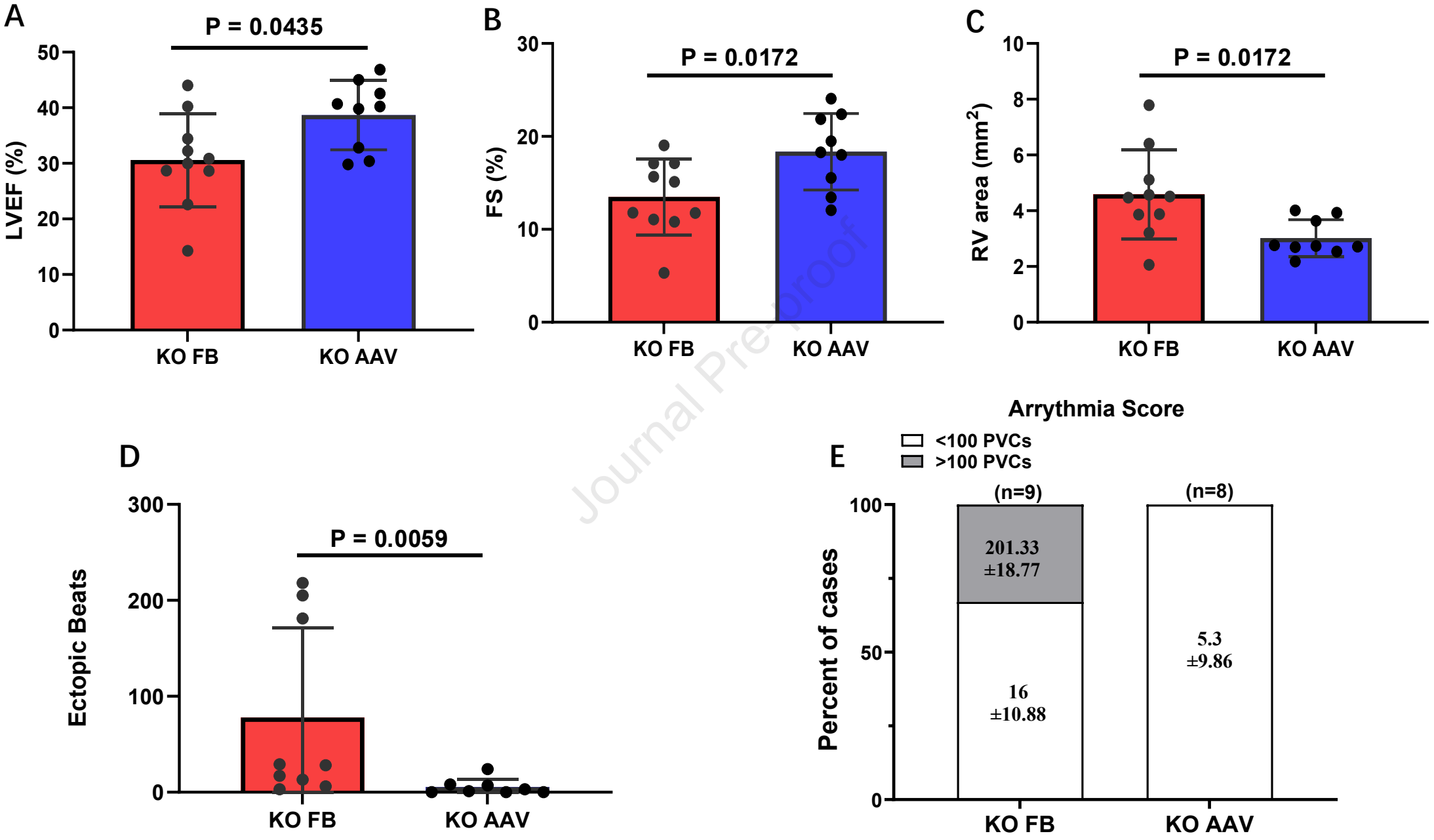

Figure 5

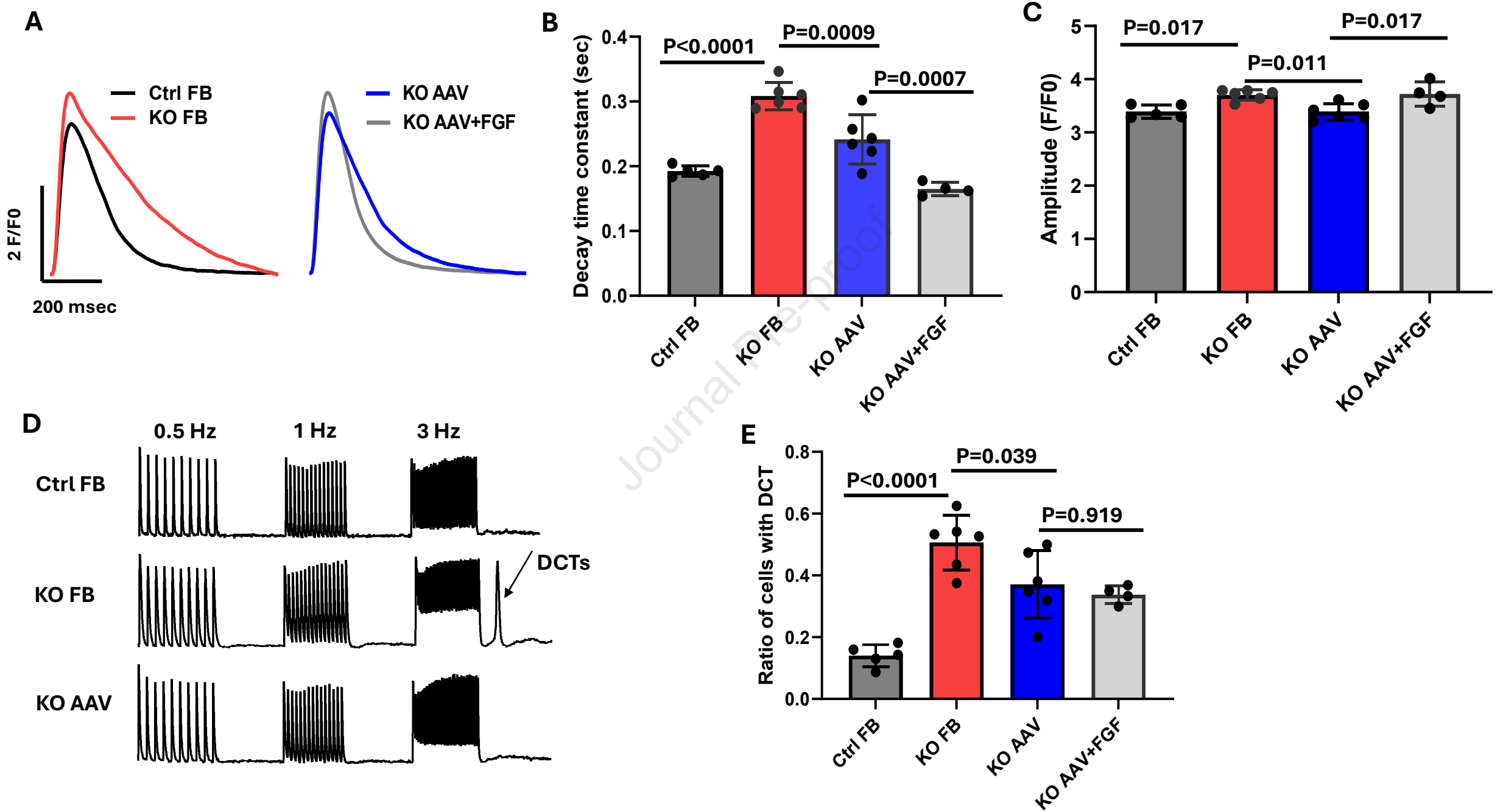

Figure 6

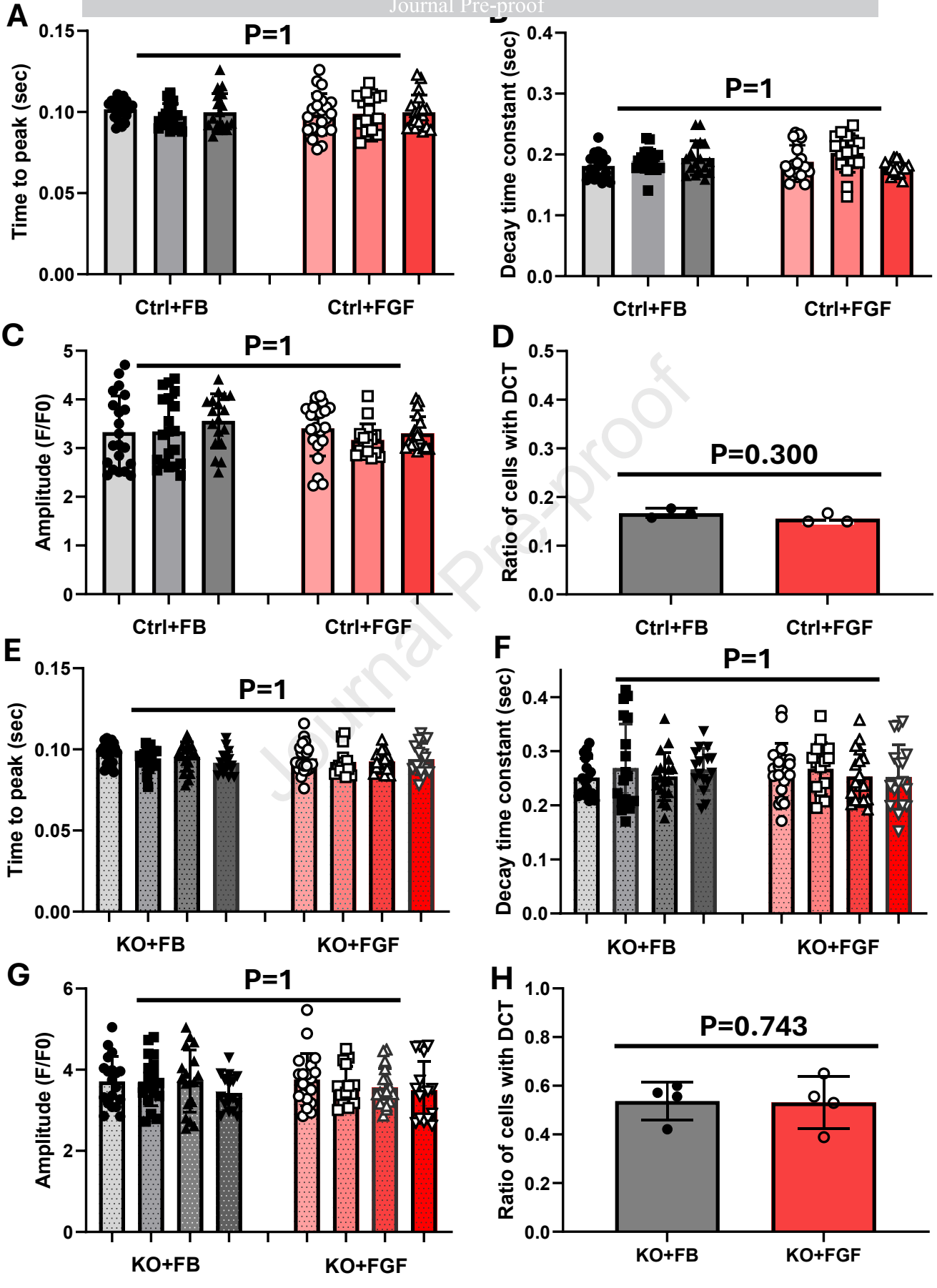

DATA SUPPLEMENTS

AAV Promoter and Cassette details.

ApoE x 3 binding

cagagaggtctctgacctctgccccagctccaaggtcagcaggcagggagggctgtgtgtttgctgtttgctgcttgcaatgtttgcccatttt
agggacatgagtaggctgaagtttgttcagtgtggacttcagaggcagcacacaaacagcaagtgtgcgatatgcagtctacagagaggtc
tctgacctctgccccagctccaaggtcagcaggcagggagggctgtgtgtttgctgtttgctgcttgcaatgtttgcccattttagggacatga
gtaggctgaagtttgttcagtgtggacttcagaggcagcacacaaacagcaaggatgcgtaatgcagtctacagagaggtctctgacctctg
ccccagctccaaggtcagcaggcagggagggctgtgtgtttgctgtttgctgcttgcaatgtttgcccattttagggacatgagtaggctgaa
gtttgttcagtgtggacttcagaggcagcacacaaacagc

hAAT promoter

atcttgctaccagtggaacagccactaaggattctgcagtgagagcagagggccagctaagtggtactctcccagagactgtctgactcac
gccacccccctccaccttggacacaggacgctgtggtttctgagccaggtacaatgactcctttcggtaagtgcagtggaagctgtacactgc
ccaggcaaagcgtccgggcagcgtaggcgggcgactcagatcccagccagtggacttagcccctgtttgctcctccgataactggggtga
ccttggttaatattcaccagcagcctcccccgttgcccctctggatccactgcttaaatacggacgaggacagggccctgtctcctcagcttca
ggcaccaccactgacctgggacagtg

bGlobin intron

gtgagtctatgggacccttgatgttttctttcccccttctttttctatggttaagttcatgtcataggaaggggagaagtaacagggtacacatattga
ccaaatcagggtaattttgcatttgtaattttaaaaaatgctttcttctttttaatatacttttttgtttatcttatttctaatactttccctaatctctttctttca
gggcaataatgatacaatgtatcatgcctctttgcaccattctaaagaataacagtgataatttctgggttaaggcaatagcaatatttctgcatat
aaatatttctgcatataaattgtaactgatgtaagaggtttcatattgctaatagcagctacaatccagctaccattctgcttttatttttatggttggg
ataaggctggattattctgagtccaagctaggccctttgctaatcatgttcatacctcttatcttcctcccacag

FGF21

atgGAATGGATGCGGTCCCGAGTGGGTACaTTGGGGCTGTGGGTGCGATTGCTTTTGG
CCGTGTTTCTCCTGGGTGTCTACCAAGCCTACCCAATTCCCGACTCAAGTCCTCTTCT
CCAATTCGGCGGTCAGGTAAGACAACGATATCTTTACACAGACGATGATCAAGATA
CAGAAGCACACCTGGAAATTAGGGAGGACGGTACTGTCGTTGGTGCCGCACATCGA

AGTCCTGAGAGTTTGCTGGAGCTCAAGGCCCTGAAACCCGGAGTGATTCAGATTTTG
GGAGTGAAGGCATCACGATTTCTGTGCCAGCAACCTGACGGCGCACTTTACGGATCA
CCTCACTTTGATCCCGAGGCCTGTTCTTTCAGAGAGTTGCTTCTCGAAGATGGATAC
AACGTATATCAGAGTGAGGCTCACGGGCTCCCCTTGCGCCTGCCCCAGAAAGACAG
TCCAAATCAAGACGCTACTTCCTGGGGTCCTGTGCGGTTCCTCCCTATGCCTGGACTT
CTGCACGAGCCACAAGACCAAGCAGGATTTCTGCCCCCAGAGCCACCCGATGTTGG
GTCTTCCGACCCTCTCTCAATGGTAGAGCCTTTGCAGGGACGATCTCCTTCCTATGCA
AGCTGA

WPRE3-Sv40

aatcaacctctggattacaaaatttgtgaaagattgactggtattcttaactatgttgctccttttacgctatgtggatacgctgctttaatgcctttgt
atcatgctattgcttcccgtatggctttcattttctcctccttgtataaatcctggttagttcttgccacggcggaactcatcgccgcctgccttgcc
cgctgctggacaggggctcggctgttgggcactgacatttatttgtgaaatttgtgatgctattgctttatttgtaaccatctagctttatttgtgaa
atttgtgatgctattgctttatttgtaaccattataagctgcaataaacaagttaacaacaacaattgcattcattttatgtttcaggttcaggggggag
atgtgggaggtttttttaaa

Raw total sequence

cagagaggtctctgacctctgccccagctccaaggtcagcaggcagggagggctgtgtgtttgctgtttgctgcttgcaatgtttgcccatttt
agggacatgagtaggctgaagtttgttcagtgtggacttcagaggcagcacacaaacagcaagtgtgcgatatgcagtctacagagaggtc
tctgacctctgccccagctccaaggtcagcaggcagggagggctgtgtgtttgctgtttgctgcttgcaatgtttgcccattttagggacatga
gtaggctgaagtttgttcagtgtggacttcagaggcagcacacaaacagcaaggatgcgtaatgcagtctacagagaggtctctgacctctg
ccccagctccaaggtcagcaggcagggagggctgtgtgtttgctgtttgctgcttgcaatgtttgcccattttagggacatgagtaggctgaa
gtttgttcagtgtggacttcagaggcagcacacaaacagcatcttgctaccagtggaacagccactaaggattctgcagtgagagcagagg
gccagctaagtggtactctcccagagactgtctgactcacgccacccccctccaccttggacacaggacgctgtggtttctgagccaggtaca
atgactcctttcggtaagtgcagtggaagctgtacactgcccaggcaaagcgtccgggcagcgtaggcgggcgactcagatcccagcca
gtggacttagcccctgtttgctcctccgataactggggtgaccttggttaatattcaccagcagcctcccccgttgcccctctggatccactgct
taaatacggacgaggacagggccctgtctcctcagcttcaggcaccaccactgacctgggacagtggtgagtctatgggacccttgatgttt
tctttccccttcttttctatggttaagttcatgtcataggaaggggagaagtaacagggtacacatattgaccaaatcagggtaattttgcatttgt
aattttaaaaaatgctttcttcttttaatatactttttgtttatcttatttctaatactttccctaatctctttctttcagggcaataatgatacaatgtatcat
gcctctttgcaccattctaaagaataacagtgataatttctgggttaaggcaatagcaatatttctgcatataaatatttctgcatataaattgtaact

gatgtaagaggtttcatattgctaatagcagctacaatccagctaccattctgcttttattttatggttgggataaggctggattattctgagtccaa
gctaggccctttgctaatcatgttcatacctcttatcttcctcccacagGCGGCCGCgccaccatgGAATGGATGCGGTC
CCGAGTGGGTACaTTGGGGCTGTGGGTGCGATTGCTTTTGGCCGTGTTTCTCCTGGGT
GTCTACCAAGCCTACCCAATTCCCGACTCAAGTCCTCTTCTCCAATTCGGCGGTCAG
GTAAGACAACGATATCTTTACACAGACGATGATCAAGATACAGAAGCACACCTGGA
AATTAGGGAGGACGGTACTGTCGTTGGTGCCGCACATCGAAGTCCTGAGAGTTTGCT
GGAGCTCAAGGCCCTGAAACCCGGAGTGATTCAGATTTTGGGAGTGAAGGCATCAC
GATTTCTGTGCCAGCAACCTGACGGCGCACTTTACGGATCACCTCACTTTGATCCCG
AGGCCTGTTCTTTCAGAGAGTTGCTTCTCGAAGATGGATACAACGTATATCAGAGTG
AGGCTCACGGGCTCCCCTTGCGCCTGCCCCAGAAAGACAGTCCAAATCAAGACGCT
ACTTCCTGGGGTCCTGTGCGGTTCCTCCCTATGCCTGGACTTCTGCACGAGCCACAA
GACCAAGCAGGATTTCTGCCCCCAGAGCCACCCGATGTTGGGTCTTCCGACCCTCTC
TCAATGGTAGAGCCTTTGCAGGGACGATCTCCTTCCTATGCAAGCTGAtaaATCGATaat
caacctctggattacaaaatttgtgaaagattgactggtattcttaactatgttgctccttttacgctatgtggatacgctgctttaatgcctttgtatc
atgctattgcttcccgtatggctttcattttctcctccttgtataaatcctggttagttcttgccacggcggaactcatcgccgcctgccttgcccgc
tgctggacaggggctcggctgttgggcactgacatttatttgtgaaatttgtgatgctattgctttatttgtaaccatctagctttatttgtgaaatttg
tgatgctattgctttatttgtaaccattataagctgcaataaacaagttaacaacaacaattgcattcattttatgtttcaggttcaggggggagatgt
gggaggtttttaaa

Supplemental Figure 1. Quantification of decay time constant (**A**), peak amplitude (**B**), and time to peak (**C**) of calcium transients from ventricular myocytes paced at 1 Hz rate. The adult female PKP2-cKO mice were injected with AAV8-FGF21(KO AAV) or its formulation buffer (KO FB), and female Cre-negative control mice were injected with FB (Ctrl FB). Each dot represents the value of one cardiomyocyte, and each bar represents the data from one animal. n=18-25 cardiomyocytes for each animal and N= 5, 6 and 6 mice for each group. SPSS Mixed model analysis.